

Current Sheet Axial Dynamics of 2.5-kJ KSU-DPF Under High-Pressure Regime

Amgad E. Mohamed, *Member, IEEE*, Ali E. Abdou, *Member, IEEE*,
Mohamed I. Ismail, *Member, IEEE*, S. Lee, and S. H. Saw

Abstract—In dense plasma focus (DPF) machines, the high-pressure (HP) regime of operation can be used as alternative technique to short-circuit (SC) test as the current sheet motion is minimal. The SC test was performed to get the right values for the static parameters of the machine. HP shots of more than 30 mbar were performed on the 2.5-kJ Kansas State University DPF machine to determine the deviation of HP values from SC values in computed static inductance and resistance. The test was performed using various gases over a wide range of molecular/atomic mass, starting from hydrogen as the lightest gas up to argon. It was found that the deviation in static inductance and resistance computed from HP method is inversely proportional to gas molecular mass at a certain pressure. The heavy gases like neon and argon were found to give the most accurate results. At 60 mbar of argon, the inductance deviation was 6.5%, and the resistance deviation was 14%. It was found also that increasing gas pressure over 30 mbar using heavy gases like Ar or Ne gives no effective improvement on the computed static impedance. Snowplow model was used to predict the axial position and the axial speed of the current sheet during the HP regime. The model showed that the average axial speed in heavy gases like argon was 0.8 cm/ μ s, whereas in hydrogen, it was 1.6 cm/ μ s.

Index Terms—Axial speed, high-pressure (HP) discharge, plasma focus, plasma resistance, snowplow model, static inductance.

I. INTRODUCTION

THE STATIC impedance of the dense plasma focus (DPF) capacitor bank is considered an important parameter in determining the behavior of the current waveform supplied to the machine. Hence, it affects the neutron yield and X-ray emission of such machine [1], [2]. The plasma focus machines of Mather type have been recently classified into two types according to the value of their static inductance [3]. The most reliable method to determine the DPF static parameters C_o , L_o , and R_o is the short-circuit (SC) test. On the other hand,

Manuscript received October 12, 2011; revised June 6, 2012; accepted July 20, 2012. Date of publication August 16, 2012; date of current version October 5, 2012. This work was supported by the Department of Mechanical and Nuclear Engineering, Kansas State University, Manhattan, KS, USA.

A. E. Mohamed, A. E. Abdou, and M. I. Ismail are with the Department of Mechanical and Nuclear Engineering, Kansas State University, Manhattan, KS 66506 USA (e-mail: engaesm@ksu.edu; aeabdou@k-state.edu; mismail1@ksu.edu).

S. Lee and S. H. Saw are with the INTI International University, 71800 Nilai, Malaysia, and also with the Institute for Plasma Focus Studies, Melbourne, VIC 3148, Australia (e-mail: leesing@optusnet.com.au; sorheoh.saw@newinti.edu).

Color versions of one or more of the figures in this paper are available online at <http://ieeexplore.ieee.org>.

Digital Object Identifier 10.1109/TPS.2012.2210738

the SC test is technically difficult to perform particularly in high-current machines, so it may be preferred to perform a high-pressure (HP) test to get approximate values for the static parameters [4]. The assumption is that, at HPs, the current sheet hardly moves as the high gas density suppresses the current sheet motion; the gas density in the HP regime is about 5–30 times more than the optimum gas work density.

The discharge current predominantly goes through diffusive ohmic regime rather than electromagnetic regime.

Although the HP gas greatly slows down the motion of the current sheet, a small displacement still exists, which adds an amount of inductance and resistance to the circuit, thus causing an overestimation of the static parameters [1].

II. KSU-DPF EXPERIMENT

A. KSU-DPF Specifications

The Kansas State University DPF (KSU-DPF) is a Mather-type geometry composed of three main parts: The capacitor bank comprises an Aerovox capacitor of 12.5- μ F capacitance with rated voltage of 20 kV and stored energy of 2.5 kJ. The capacitor is charged using a General Atomics power supply with rated voltage of 30 kV and 8 kJ/s. The capacitor is connected to the electrodes through a thyatron TDI1–200 k/25 kV, 10-ns jitter.

The central anode is a semihollow copper rod with 100-mm active length and outer diameter of 15 mm. The anode is surrounded by a squirrel-cage cathode made of six equally spaced rods at a distance of 29 mm from the center of anode. The anode base is insulated from the cathode using a Pyrex tube of 68-mm length and 1.6-mm wall thickness. Both cathode and anode are mounted inside a stainless steel chamber with two glass windows.

The current is measured using a Rogowski coil in the dI/dt mode and then numerically integrated to obtain the current waveform. A Northstar High Voltage probe HV5 60/100 kV DC/AC 80 MHz was used to measure the voltage waveform across the tube.

B. Rogowski Coil Considerations

The discharge current waveform obtained from the numerically integrated Rogowski coil signal shows baseline shift as shown in Fig. 1. Electromagnetic pickup and power line interference are potential root causes of the baseline shift

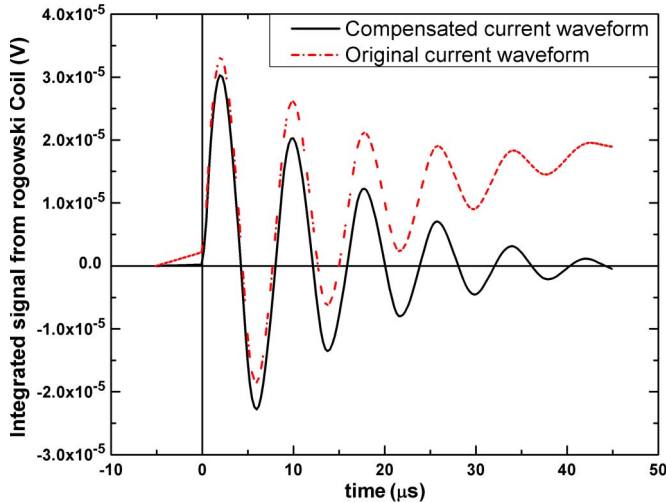


Fig. 1. Rogowski coil integrated signal, with and without compensation.

[5]; the offset could also result from grounding problems or nonsymmetrical topology effects with the mounting of the coil so that the coil monitors not only the current that passes inside but also the current that passes outside the coil [6].

Three numerical methods were introduced to resolve the problem. The first method uses a combination of digital filters on the original dI/dt coil signal. Origin program was used to perform such processing.

The second method is to find the average of the signal envelope; this technique was performed by fitting the positive peaks of the waveform as well as the negative peaks then calculating the average of both fitted curves. Afterwards, this average curve was subtracted from the original waveform. The third method was performed by capturing the first few microseconds before the signal rises and the final few microseconds close to the end of the damped curve. The time space in between the two portions was interpolated, and the interpolated curve represents the base shift. Hence, it was subtracted from the original waveform to obtain the compensated current without the baseline shift. The first and last methods gave better prediction to the baseline shift; Fig. 1 shows the original and the compensated curves using the first method.

C. HP Regime

The optimum working pressure for KSU-DPF machine is about 4 mbar in deuterium and 2 mbar for neon. The HP regime was performed under pressure range of 30–60 mbar. The capacitor is charged to 17 kV. The working gases were argon, neon, helium, deuterium, and hydrogen.

The current waveform was measured using Rogowski coil and then analyzed using the RLC analysis [1]. The resulting values for the inductance and resistance incorporate contributions due to the motion of the current sheet.

This motion has a dependence on the pressure and gas molecular weight. By studying the results in the various gases, this extraneous contribution may be more readily understood and eliminated.

III. EXPERIMENTAL WORK

An SC test was performed first to find the static parameters of the machine. A special connector was machined with a diameter and length equal to the anode base. The connector was used to connect the anode and cathode plates and compensate the impedance change due to the removal of the real anode and cathode.

HP tests were performed to determine the machine static parameters; the original anode and cathode were returned back during the test. The chamber was filled with various gases at pressures from 30–60 mbar with 10-mbar increment step. A fast response Rogowski coil was fabricated to pick up the current signal. The capacitor was charged every shot to 17 kV, and then, the shot was performed by turning on the thyatron switch. The current then flowed from the anode to the cathode through the gas medium in between. The experiment was repeated three times at each pressure to avoid inconsistent shots.

IV. THEORETICAL MODEL

The snowplow model was used to simulate the motion of the current sheet during the axial phase and to calculate the inductance induced during the current sheet motion [7].

Assuming 1-D model, with a planar current sheet perpendicular to the axis of the electrodes, this approximation is nearly true at HP [8], [9]. The change of momentum equation due to the force from ($J \times B$)

$$\begin{aligned} \frac{dmv_z}{dt} &= \frac{d}{dt} \left[f_m \rho \pi (b^2 - a^2) z(t) \frac{dz(t)}{dt} \right] \\ &= \int_a^b \frac{\mu (f_c I)^2 2\pi r dr}{2(2\pi r)^2} \end{aligned} \quad (1)$$

where a and b are the radii of the anode and cathode, respectively, ρ is the initial gas density of gas, μ is the permeability of the free space, and f_m and f_c are the snowplow mass swept-up factor and current factor, respectively.

Therefore

$$z(t) \frac{dz(t)}{dt} = \frac{\mu \ln \left(\frac{b}{a} \right)}{4\pi^2 f_m \rho (b^2 - a^2)} \int (f_c I)^2 dt. \quad (2)$$

Let $I_{\text{norm}} = I/I_0$, the normalized current waveform, integrate to find the displacement of the current sheet $z(t)$

$$z(t) = \sqrt{2U} \left(\int \left(\int I_{\text{norm}}^2 dt' \right) dt \right)^{\frac{1}{2}} \quad (3)$$

where

$$U = \sqrt{\frac{\mu \ln (b/a) (f_c I_0)^2}{4\pi^2 (f_m \rho) (b^2 - a^2)}} \quad (4)$$

is the characteristic axial transient speed from which the axial speed will be

$$\frac{dz}{dt} = \frac{U^2}{z} \int I_{\text{norm}}^2 dt. \quad (5)$$

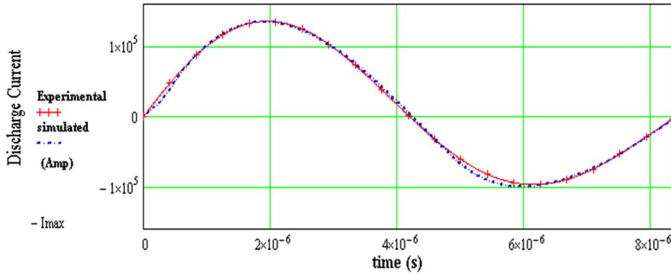


Fig. 2. Simulated current and the experimental current for deuterium at 40 mbar.

The theoretical current was calculated as sinusoidal wave modified by a damping function $I(t) = I_0 e^{-\alpha t} \sin(\omega t)$, where α is the exponential damping coefficient ($R_o/2L_o$), ω is the natural angular frequency ($\sqrt{\omega_d^2 - \alpha^2}$), and ω_d is the resonant radian frequency ($1/\sqrt{L_o C_o}$). The theoretical current was matched to the experimental current waveform by changing three factors: the frequency ω , the damping factor α , and amplitude I_0 , see Fig. 2. The current waveform, the capacity for the capacitor, and the charged voltage supplied to the circuit were used to calculate the impedance of the circuit, and these calculations can be obtained from SC analysis. Hence, the axial position and axial speed can be calculated as a function of time

$$z(t) = \frac{U}{2\alpha(\alpha^2 - \omega^2)} \times (\alpha^4 e^{-2\alpha t} (1 - \cos(2\omega t)) + \alpha^2 \omega^2 e^{-2\alpha t} (2 + \cos(2\omega t)) + 2\alpha^3 \omega e^{-2\alpha t} \sin(2\omega t) + \omega^4 (e^{-2\alpha t} - 1) - 3\alpha^2 \omega^2 + 2\alpha^3 \omega^2 t + 2\alpha \omega^4)^{\frac{1}{2}}. \quad (6)$$

The axial speed will be

$$\frac{dz(t)}{dt} = \frac{U^2}{4z(t)} \left(\frac{1 - e^{-2\alpha t}}{\alpha} + \frac{\alpha e^{-2\alpha t} \cos(2\omega t)}{(\alpha^2 + \omega^2)} - \frac{\omega e^{-2\alpha t} \sin(2\omega t) + \alpha}{(\alpha^2 + \omega^2)} \right). \quad (7)$$

Therefore, the tube inductance due to the motion of current sheet can be determined as a function of the position

$$L_p = \frac{\mu_o}{4\pi} \ln \left(\frac{b}{a} \right) Z(t). \quad (8)$$

The model was applied to previous experimental data from the literature [8]–[10]. These works assumed approximate sinusoidal current waveform $I(t) = I_0 \sin(\omega_n t)$ without the damping effect. Our damped model illustrated more precise matching than those experimental data in axial position and axial speed calculations.

V. RESULTS

A. Experimental Results

The SC test parameters were picked up from the KSU-DPF machine; for capacitor with $C_o = 12.5 \mu\text{F}$ and $V_o = 17 \text{ kV}$,

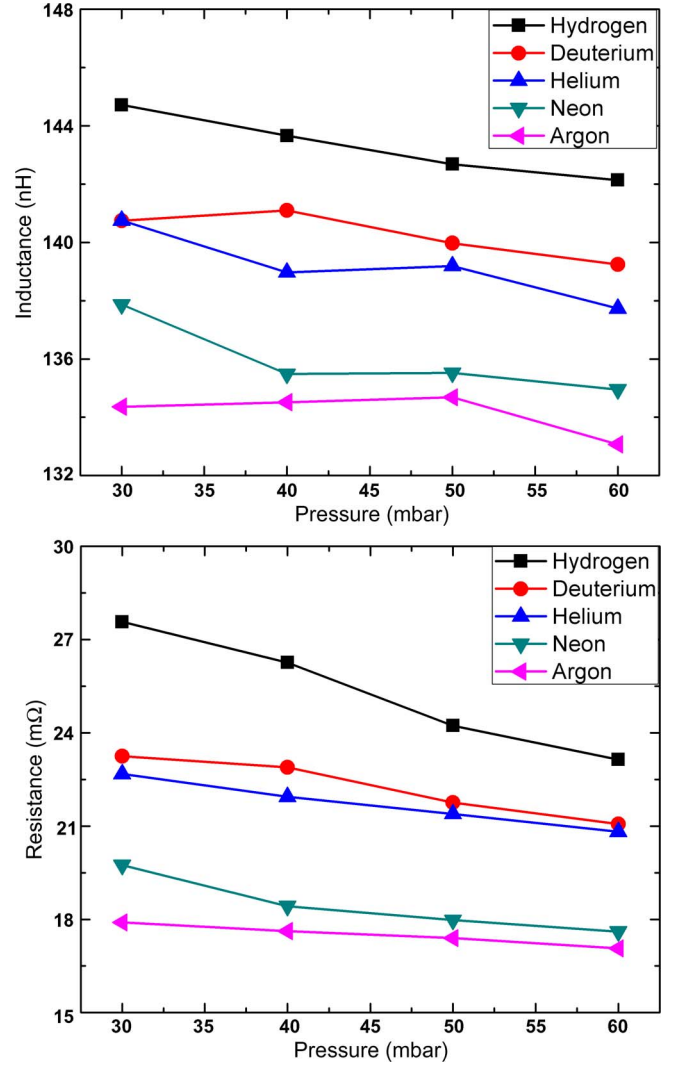


Fig. 3. Calculated resistance and inductance from the RLC model versus pressure.

the reversal ratio is $f = 0.7974$, and the periodic time is $T = 7.852 \times 10^{-6} \text{ s}$. Therefore, $L_o = 125 \text{ nH}$, $R_o = 14.4 \text{ m}\Omega$, and $I_o = 153 \text{ kA}$. Then, the Rogowski calibration factor (I_o/V_1) = $4.76 \times 10^9 \text{ A/V}$, where V_1 is the first peak of Rogowski integrated signal corresponding to the current peak I_o .

The current waveforms from the HP tests were analyzed using RLC circuit analysis as stated before. The results show noticeable difference in inductance and resistance. This difference was dropping as the pressure increased Fig. 3, particularly in light gases. The minimum calculated inductance and resistance recorded at 60-mbar argon were 133 nH and 17.1 mΩ, respectively. The maximum values recorded at 30-mbar hydrogen were 145 nH and 27.6 mΩ.

This shows that the motion of current sheet is greater in light gases than in the heavy gases. The difference in between HP and SC results was considered as a deviation in L and R when using HP method as an approximation to find the static parameters. This deviation was calculated as a function of molecular mass of the working gas. Fig. 4 shows the deviation percentage of resistance and inductance at 60 mbar; it was found that the deviation percentage was inversely proportional

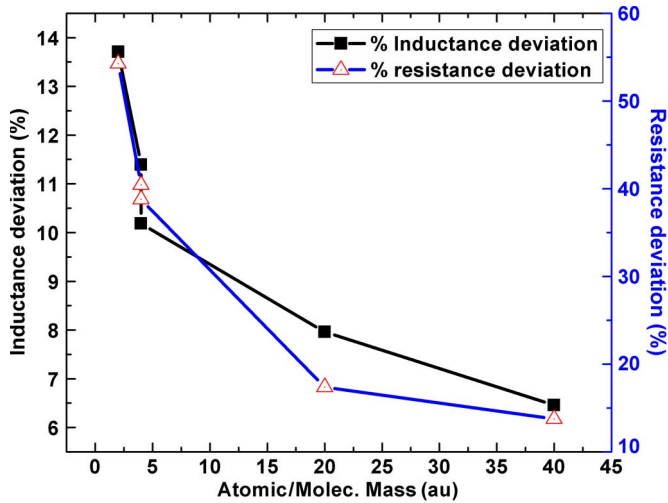


Fig. 4. HP inductance and resistance deviation versus the molecular mass of the used gas (at 60 mbar).

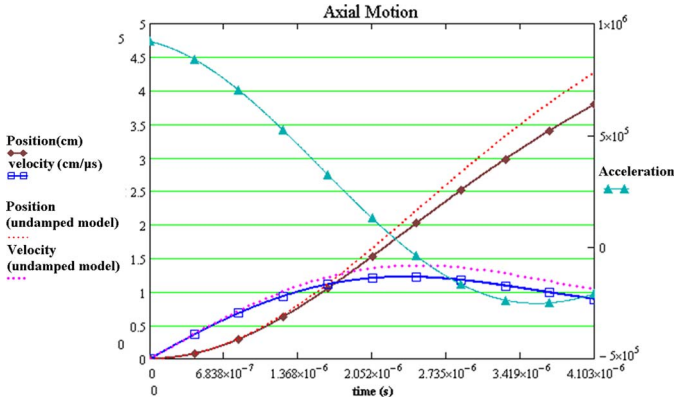


Fig. 5. Snowplow model using MathCAD dynamic sheet. Solid lines indicate the damped current model, and the dotted lines indicate the sinusoidal current model. (Data for neon at 40 mbar, 17 kV).

to the molecular mass. At 60 mbar, the deviation in calculated inductance varied from 14% for hydrogen to 6.5% for argon. The resistance deviation at the same conditions varied from 54% for hydrogen to 13.7% for argon.

B. Theoretical Model Results

Snowplow model was used to plot the axial position, speed, and acceleration in the HP regime. Fig. 5 shows the axial parameter output. The solid lines express results from the damped sinusoidal current model, and the dotted lines express the nondamped sinusoidal current model. These curves are corresponding to the first half cycle of the current waveforms. The model results indicated differences in axial position of about 30% and in speed of 15% between the two cases of current waveforms. Table I indicates the tube inductance (which is the SC inductance less the total inductance during plasma motion), corresponding axial position, and speed in various cases. The average axial speed was calculated for each gas on the range of the worked pressure. The average speed in the HP varies from 0.79 cm/μs in argon to 1.60 cm/μs in hydrogen.

TABLE I
AVERAGE AXIAL POSITION AND AXIAL SPEED
VALUES AT DIFFERENT PRESSURES

Gas	Pressure (mbar)	tube inductance Lp (nH)	Z (cm)	V (cm/μs)	Average speed (cm/μs)
Argon	60	7.36	2.83	0.70	0.79
	50	8.95	3.44	0.84	
	40	8.7	3.35	0.82	
	30	8.56	3.30	0.80	
Neon	60	9.32	3.58	0.87	0.96
	50	9.91	3.81	0.93	
	40	9.85	3.79	0.92	
	30	12.22	4.70	1.13	
Helium	60	12.20	4.70	1.13	1.25
	50	13.5	5.17	1.24	
	40	13.25	5.20	1.26	
	30	15.0	5.70	1.37	
Deuterium	60	13.39	5.15	1.23	1.32
	50	14.22	5.47	1.31	
	40	14.48	5.57	1.33	
	30	15.19	5.84	1.40	
Hydrogen	60	16.7	6.43	1.52	1.60
	50	17.09	6.58	1.55	
	40	17.7	6.80	1.60	
	30	19.18	7.38	1.732	

VI. CONCLUSION

At the HP regime, the KSU-DPF is operating at low shock wave speed; in such regime, the coupling of energy provided to the plasma is predominantly through diffusive electrical discharge rather than electromagnetic pistonlike. Nevertheless, the data do indicate that there is downstream motion of the diffusive structure which we interpret as due to electromagnetic drive. Moreover, the data for the average speed are found to be proportional to $(1/\rho)^{0.5}$ extending to the highest pressures which indicates that the speeds can be considered as electromagnetically driven even though we know that the diffusive structure is electrically resistive. This interpretation is, in a gross sense, valid as evident from our analysis which shows in every case a significantly larger inductance and resistance from the HP tests when compared with the SC tests. We are therefore presenting this technique as a useful alternative method to the SC test in order to find out the static parameters for the machine. The induced error percentage due to the motion of current sheet was calculated using the approximate model. These results can be used as a reasonable first-order correction to the values calculated with HP tests and can be applied fairly on other machines with different geometries and energy scales. Under the HP regime, it was found that the speed of the current sheet is approximately one-fifth the optimum speed in the normal working conditions. The deviation in L and R is proportional also to $(1/\rho)^{0.5}$ where ρ is the gas density.

Finally, it should be noted that, although the use of the damped sinusoidal current in the snowplow equation of motion produces more accurate results than the use of an undamped

sinusoidal current, it is still an approximation when compared to the method of using the equation of motion coupled to the circuit equation. The coupled-equation method allows for the motion and the current to be derived as the two solutions of the two-equation system. The nature of the problem is such that the current waveform is a damped sinusoid with nonlinear time-varying damping factor as well as frequency; these are correctly incorporated into the point-by-point solutions as the coupled equations are numerically solved [1], [11]. Nevertheless, the use of a damped sinusoidal current in the equation of motion may still be used as a simpler alternative for analytical purposes.

REFERENCES

- [1] S. H. Saw, S. Lee, F. Roy, P. L. Chong, V. Vengadeswaran, A. S. M. Sidik, Y. W. Leong, and A. Singh, "In situ determination of the static inductance and resistance of a plasma focus capacitor bank," *Rev. Sci. Instrum.*, vol. 81, no. 5, pp. 053505-1–053505-4, 2010.
- [2] W. A. Bernard, H. Bruzzone, P. Choi, H. Chuaqui, V. Gribkov, J. Herrera, K. Hirano, A. Krejci, S. Lee, C. Luo, F. Mezzetti, M. Sadowski, H. Schmidt, K. Ware, C. S. Wong, and V. Zoita, "Scientific status of plasma focus research," *Moscow J. Phys. Soc.*, vol. 8, no. 2, pp. 93–170, 1998.
- [3] S. Lee, S. Saw, A. Abdou, and H. Torreblanca, "Characterizing plasma focus devices—Role of the static inductance—Instability phase fitted by anomalous resistances," *J. Fusion Energy*, vol. 30, no. 4, pp. 277–282, 2011.
- [4] S. S. Lee, "Experiments with the ICTP-UM 3.3 kJ plasma fusion facility," *Spring College Plasma Phys., Int. Centre Theor. Phys., Trieste, Italy*, May 27–Jun. 22, 1991.
- [5] D. A. Ward and J. L. T. Exon, "Using Rogowski coils for transient current measurements," *Eng. Sci. Educ. J.*, vol. 2, no. 3, pp. 105–113, Jun. 1993.
- [6] S. Lee, S. Saw, R. Rawat, P. Lee, R. Verma, A. Talebitaher, S. Hassan, A. Abdou, M. Ismail, A. Mohamed, H. Torreblanca, S. Al Hawat, M. Akel, P. Chong, F. Roy, A. Singh, D. Wong, and K. Devi, "Measurement and processing of fast pulsed discharge current in plasma focus machines," *J. Fusion Energy*, vol. 31, no. 2, pp. 198–204, 2012.
- [7] L. R. M. G. (1978, Sep.). A comment on the shape of the current sheet in a coaxial accelerator. *J. Phys. D.* [Online]. 11(13), pp. 1911–1916. Available: <http://stacks.iop.org/0022-3727/11/i=13/a=013>
- [8] M. Mathuthu, T. G. Zengeni, and A. V. Gholap, "Measurement of magnetic field and velocity profiles in 3.6 kJ United Nations University/International Center for theoretical physics plasma focus," *Phys. Plasmas*, vol. 3, no. 12, pp. 4572–4576, 1996.
- [9] S. Al-Hawat, "Axial velocity measurement of current sheath in a plasma focus device using a magnetic probe," *IEEE Trans. Plasma Sci.*, vol. 32, no. 2, pp. 764–769, Apr. 2004.
- [10] H. Bhuyan, S. R. Mohanty, N. K. Neog, S. Bujarbarua, and R. K. Rout, "Magnetic probe measurements of current sheet dynamics in a coaxial plasma accelerator," *Meas. Sci. Technol.*, vol. 14, no. 10, pp. 1769–1776, Oct. 2003.
- [11] RADPF, S. Lee, Radiative Dense Plasma Focus Computation Package, 2011. [Online]. Available: www.intimal.edu.my/school/fas/UFLF/

Amgad E. Mohamed (M'03) received the B.Sc. (Hons.) degree in electrical engineering and the M.Sc. degree in engineering physics from Zagazig University, Zagazig, Egypt, in 2000 and 2007, respectively. He is currently working toward the Ph.D. degree in nuclear engineering in the Department of Mechanical and Nuclear Engineering, Kansas State University, Manhattan.

He has experience in low-temperature plasmas and dense plasma focus.

Ali E. Abdou (M'03) received the B.S. degree in nuclear engineering from Alexandria University, Alexandria, Egypt, in 1992 and the M.S. degree in nuclear engineering, the M.S. degree in computational sciences, and the Ph.D. degree in nuclear engineering from the University of Wisconsin, Madison, in 2002, 2003, and 2005, respectively.

He has over 15 years of experience in the nuclear science and engineering fields. From 1994 to 1999, he participated in the design, preoperation, inauguration, and operation of Egypt's second test and research nuclear reactor ETRR-2. From 2005 to 2009, he was a Senior Process Development Engineer with Portland Technology Development, Intel Corporation, where he worked in the area of plasma etching and semiconductor nanofabrication. He was responsible for the process development of shallow trench isolation for 65-, 45-, and 32-nm nodes. He has wide expertise in plasma processing techniques used in the fabrication and characterization of semiconductor nano-/microstructures. Since early 2009, he has been with the Department of Mechanical and Nuclear Engineering, Kansas State University, Manhattan, as an Assistant Professor of nuclear engineering. He has authored or coauthored over 48 research publications. His current research interests include the development of nanosecond compact multiradiation sources based on the dense plasma focus, the research and development of plasma etching in semiconductor nanofabrication, optical emission spectroscopy, and X-ray emission from plasmas.

Dr. Abdou was a recipient of the licenses in radiation protection from Argentinean ENRN and in health physics from Egyptian NRC in 1996 and 1997, respectively.

Mohamed I. Ismail (M'03) received the B.Sc. degree in electrical engineering and the M.Sc. degree in engineering physics from Zagazig University, Zagazig, Egypt, in 1999 and 2007, respectively. He is currently working toward the Ph.D. degree in nuclear engineering in the Department of Mechanical and Nuclear Engineering, Kansas State University, Manhattan.

His main research interests include plasma diagnostics and dense plasma focus.

S. Lee received the B.Sc. and M.Sc. degrees from the University of Malaya (UM), Kuala Lumpur, Malaysia, in 1964 and 1966, respectively, and the Ph.D. degree from the Australian National University, Canberra, Australia, in 1970.

He was a Professor of applied physics, headed research groups in plasma and pulse technology and the Department of Physics, UM, and was the Head with the Division of Physics and the Head Academic Group of Natural Sciences, National Institute of Education, Nanyang Technological University, Singapore, Singapore. He was an Alexander von Humboldt Fellow with Kernforschungslange, Juelich, Germany, from 1975 to 1976, a Commonwealth Academic Staff Fellow with Imperial College London, London, U.K., from 1981 to 1982, and a Visiting Professor and a United Nations University Special Fellow with Flinders University, Adelaide, Australia, from 1986 to 1987. He is currently an Adjunct Professor (honorary) of INTI International University, Nilai, Malaysia. He is also currently the Founding Director of the (Web-based) Institute for Plasma Focus Studies, Melbourne, Australia.

Dr. Lee was the Founder President of Asian African Association for Plasma Training (AAAPT); the Associate Director of the AAAPT Research and Training Center, Institute of Physics, Academia Sinica, Beijing, China; a Far Eastern Representative of the International Center for Theoretical Physics; and an ardent advocate and an implementor of south–south technology creation and transfer, in plasma fusion, laser, and pulse technology. He is also a Chartered Physicist and a fellow of the Institute of Physics, U.K., a life and honorary fellow of the Institute of Physics, Malaysia, a life fellow of Singapore Institute of Physics and the Samahang Pisika ng Pilipinas, and an honorable member of the Turkish Science and Research Foundation TUBAV.

S. H. Saw received the B.Sc. (Hons.) and Ph.D. degrees in physics from the University of Malaya, Kuala Lumpur, Malaysia, in 1985 and 1991, respectively, and the M.A. degree in educational management from The University of Nottingham, Nottingham, U.K., in 1997.

She is currently a Professor and the Pro-Vice-Chancellor for education quality and innovation with INTI International University (INTI IU), Nilai, Malaysia, where she is the Director of the Center for Plasma Research. She is the Codirector with the Institute for Plasma Focus Studies, Melbourne, Australia, and the designated delegate of INTI IU for the Asian African Association for Plasma Training. Her current research interests include plasma physics and innovation in education.

Dr. Saw was conferred an honorary membership of the Turkish Science and Research Foundation TUBAV in 2009.